High Pressure NMR Reveals Active-Site Hinge Motion of Folate-Bound *Escherichia coli* Dihydrofolate Reductase†

Ryo Kitahara,§ Sina Sareth,§ Hiroaki Yamada,⊥ Eiji Ohmae,‖ Kunihiko Gekko,‖ and Kazuyuki Akasaka*,§,⊥

Department of Molecular Science, Graduate School of Science and Technology, and Department of Chemistry, Faculty of Science, Kobe University, 1-1 Rokkodai-cho, Nada-ku, Kobe 657-8501, Japan, and Department of Mathematical and Life Sciences, Graduate School of Science, Hiroshima University, Higashi-Hiroshima 739-8526, Japan

Received May 1, 2000; Revised Manuscript Received July 31, 2000

ABSTRACT: A high-pressure $^{15}N/^{1}H$ two-dimensional NMR study has been carried out on folate-bound dihydrofolate reductase (DHFR) from *Escherichia coli* in the pressure range between 30 and 2000 bar. Several cross-peaks in the $^{15}N/^{1}H$ HSQC spectrum are split into two with increasing pressure, showing the presence of a second conformer in equilibrium with the first. Thermodynamic analysis of the pressure and temperature dependencies indicates that the second conformer is characterized by a smaller partial molar volume ($\Delta V = -25$ mL/mol at 15 °C) and smaller enthalpy and entropy values, suggesting that the second conformer is more open and hydrated than the first. The splittings of the cross-peaks (by ∼1 ppm on ^{15}N axis at 2000 bar) arise from the hinges of the M20 loop, the C-helix, and the F-helix, all of which constitute the major binding site for the cofactor NADPH, suggesting that major differences in conformation occur in the orientations of the NADPH binding units. The Gibbs free energy of the second, open conformer is 5.2 kJ/mol above that of the first at 1 bar, giving an equilibrium population of about 10%. The second, open conformer is considered to be crucial for NADPH binding, and the NMR line width indicates that the upper limit for the rate of opening is 20 s^{-1} at 2000 bar. These experiments show that high pressure NMR is a generally useful tool for detecting and analyzing "open" structures of a protein that may be directly involved in function.

Enzymatic function is intimately related to the ability of a protein to adopt conformations suitable for binding a substrate and a cofactor. Dihydrofolate reductase (DHFR)[1] catalyzes the NADPH-linked reduction of 7,8-dihydrofolate to 5,6,7,8-tetrahydrofolate and has a cofactor binding pocket and a substrate binding pocket. *Escherichia coli* DHFR assumes a variety of conformations in crystals, depending on whether it binds the substrate (or a substrate analogue), the cofactor, or both (*1*). These conformations are classified into three major conformations: "open", "closed", and "occluded". The closed conformations refer to the conformations that the DHFR assumes when complexed with cofactor NADPH, the occluded conformations refer to the conformations of the DHFR in which the nicotinamide binding pocket is occluded by the M20 loop, and the open conformations refer to conformations of the DHFR in which the NADPH binding site is open (*1*). Sawaya and Kraut have used the structural differences among these conformers in crystals to explain the enzyme's conformational changes in the catalytic cycle (*1*).

In the folate-bound form of the DHFR, two conformations have been reported in crystals, open and occluded, with a large difference in the orientation of the M20 loop and in the orientation in the C and F helices. However, only one conformation has been reported in solution by NMR spectroscopy (*2*), which, however, shows the existence of significant slow conformational fluctuations in the folate-binding regions including the M20 loop (*2*). In the case of the complex of *E. coli* DHFR with methotrexate, a transition-state analogue of dihydrofolate, the existence of two conformers has been clearly demonstrated from the side chain signals in ^{1}H NMR (*3*). In apo DFHR also, two conformations have been detected, which differ in the M20 and FG loops (*4*, *5*). These observations indicate that DHFR can assume multiple conformations in solution, the detailed knowledge of the structures and thermodynamics of which may be crucial to understand its reaction mechanism.

The online variable pressure cell NMR technique (*6*) has emerged as a novel means of detecting site-specific conformational changes of proteins in solution under variable pressure (*7*−*12*). In particular, it enables detection of "hidden" equilibrium conformational species of proteins by utilizing differential partial volumes among conformers of proteins rather than utilizing differential thermal, pH, or denaturant stability (*12*). In the present work, the solution conformation of the folate-bound form of the ^{15}N-uniformly

† This work was supported by Grants-in-Aid for Scientific Research from the Ministry of Education, Science, Sports and Culture of Japan (#10480159 and #12480201). This work is supported by a JSPS postdoctoral fellowship to S.S.

* To whom correspondence should be addressed. Phone: +81-78-803-5687. Fax: +81-78-803-5688. E-mail: akasaka@kobe-u.ac.jp.

§ Department of Molecular Science, Kobe University.

⊥ Department of Chemistry, Kobe University.

‖ Hiroshima University.

[1] Abbreviations: DHFR, dihydrofolate reductase; $NADP^{+}$ and NADPH, nicotinamide adenine dinucleotide phosphate (oxdized and reduced, respectively); NMR, nuclear magnetic resonance; HSQC, heteronuclear single-quantum coherence; DSS, 2,2-dimethyl-2-silapentane-5-sulfonate.

10.1021/bi0009993 CCC: $19.00
Published on Web 09/27/2000

labeled *E. coli* DHFR has been studied as a function of pressure at individual backbone amides by utilizing the online variable pressure cell NMR technique (*6*). $^{15}N/^{1}H$ two-dimensional HSQC NMR spectra were recorded in the pressure range between 30 and 2000 bar. The result revealed that the folate-bound DHFR undergoes a hinge motion in the NADPH binding sites, opening and closing the active site, which is considered to be crucial for the catalytic activity of the DHFR.

MATERIALS AND METHODS

Sample Preparation. ^{15}N-labeled DHFR was obtained from *E. coli* strain BL21 with the plasmid pTP64-1 (*13*). A modified M9 minimal medium containing 4 g of glucose, 1 g of ^{15}N-ammonium sulfate, 1.6 g of sodium chloride, and 20 mg of trimethoprim/L was used for producing ^{15}N-labeled DHFR. The protein was purified by the method described previously (*14*), concentrated by a Centricut mini V-10 ultrafiltration membrane (Kurabo Industries Ltd., Tokyo), and then dialyzed against 20 mM Tris buffer (pH 7.0). Incorporation of ^{15}N isotopes into the protein was checked by mass spectrometry (JMS-SX102A/ESI10HS, JEOL). The mass number of ^{15}N-labeled DHFR was larger by 218 than that of the nonlabeled DHFR, indicating that all nitrogen atoms were substituted with ^{15}N. The final protein concentration was adjusted to be 1.2 mM in 20 mM Tris buffer (pH 7.0) containing 4.5 mM folate and 5% $^{2}H_2O$. The protein concentration was determined spectrophotometrically using a molar extinction coefficient of 31 100 M^{-1} cm^{-1} at 280 nm (*15*).

High-Pressure NMR Measurements. The high-resolution, high-pressure NMR technique is a modification of the online high pressure glass tube method originally reported by Yamada (*6*). The protein solution is contained in a quartz tube (inner diameter less than 1 mm, outer diameter of ~3 mm, protected by a Teflon jacket), which is separated from the pressure mediator (kerosene) by Teflon pistons in a separator cylinder (BeCu). Pressure was controlled between 1 and 2000 bar with a hand pump. NMR spectra were measured on a Bruker DMX-750 spectrometer operating at a proton frequency of 750.13 MHz and a ^{15}N frequency of 76.01 MHz. The $^{15}N/^{1}H$ HSQC spectra were measured with a standard HSQC sequence (*16*) combined with a WATERGATE technique with a 3-9-19 pulsed field gradient (*17*). The ^{15}N dimension was acquired with 256 increments and for the proton dimension 2048 complex points were collected with an offset at the residual water signal. At all pressures, ^{1}H chemical shifts were referenced to the methyl signal of 2,2-dimethyl-2-silapentane-5-sulfonate (DSS) and ^{15}N chemical shifts were indirectly referenced to DSS (0 ppm) and dioxane (3.75 ppm). The chemical shift difference between DSS and dioxane was invariant with pressure within experimental error. The pH change of the Tris buffer solution at 2000 bar is estimated to be within 0.1 pH units from the known ionization volume of Tris (*18*). Data were processed with the UXNMR package (Bruker) running on a Silicon Graphics O2 workstation. Spectra were zero-filled to give a final matrix of 2048 × 512 real data points and apodized with a shifted sine-bell (90°) window function in both dimensions.

Calculations of Thermodynamic Parameters. Equilibrium constants K were obtained for the equilibrium between the two conformers of folate-bound DHFR from cross-peak intensities (volumes) of the respective conformers in HSQC spectra as a function of pressure and temperature. Gibbs free energy differences (ΔG) between the two conformers are given by eq 1 as a function of pressure p at constant temperature T and by eq 2 as a function of temperature at constant pressure:

$$\Delta G = -RT \ln K = \Delta G_0 - (p - p_0)\Delta V \quad (1)$$

$$\Delta G = -RT \ln K = \Delta H - T\Delta S \quad (2)$$

Here R is the gas constant, T is the absolute temperature, ΔG_0 is the Gibbs free energy difference at p_0 (= 1 bar), ΔV is the difference in the partial molar volume, ΔH is the difference in enthalpy, and ΔS is the difference in entropy. Thermodynamic parameters, ΔG_0, ΔV, ΔH, and ΔS, were obtained by least-squares fit of experimental data to eqs 1 and 2.

RESULTS

Figure 1 shows the $^{15}N/^{1}H$ HSQC spectra of uniformly ^{15}N-labeled DHFR at 30 bar (blue) and at 2000 bar (red). Cross-peaks corresponding to 159 amino acid residues were detected, out of which 100 cross-peaks are assigned to individual amide groups by referring to assignments in the literature (*19*, *20*). All cross-peaks undergo continuous shifts with pressure; all signals are followed in the pressure range of 30 to 2000 bar, making assignments at 2000 bar relatively straightforward. However, several cross-peaks split into two at 2000 bar (Figure 1, encircled cross-peaks), which originate from Arg12, Val13, Trp22, Gly51, and Gly95. In addition, some cross-peaks lose intensity or disappear completely at 2000 bar.

Figure 2 shows intensity changes of the split cross-peaks as a function of pressure and temperature for Val13-NH and Trp22-NϵH. Clearly, the second (new) cross-peak increases apparently at the expense of the first (original) cross-peak with increasing pressure at each temperature and with decreasing temperature at constant pressure. Similar spectral changes were observed for the NH's of Trp22, Gly51, and Gly95. On average, the chemical shift of the second cross-peak, relative to the first, is ~1 ppm (to the low field, except for Gly51) in the ^{15}N axis and within ~0.4 ppm (to the high field, except for Arg12) in the ^{1}H axis. The shifts are larger than the average pressure-induced shifts in globular proteins, for example, 0.468 and 0.075 ppm/2000 bar for ^{15}N and ^{1}H, respectively, in BPTI (*9*).

In Figure 3A, the normalized intensities of the paired split cross-peaks are plotted as a function of pressure for the five residues, Arg12, Val13, Trp22 (both main chain and side chain), Gly51, and Gly95. For each pair, the total intensity remains almost constant with pressure, suggesting an equilibrium between two conformers. Since the cross-peak intensity is proportional to the population of the conformer, we can calculate the equilibrium constant for each pair as a function of pressure. The equilibrium constants for the five residues behave more or less similar against pressure (see Figure 3A), showing that the local conformational changes at the five residue sites are likely to be governed by a cooperative transition. By taking the average equilibrium constant of the five residues in Figure 3A and replotting its

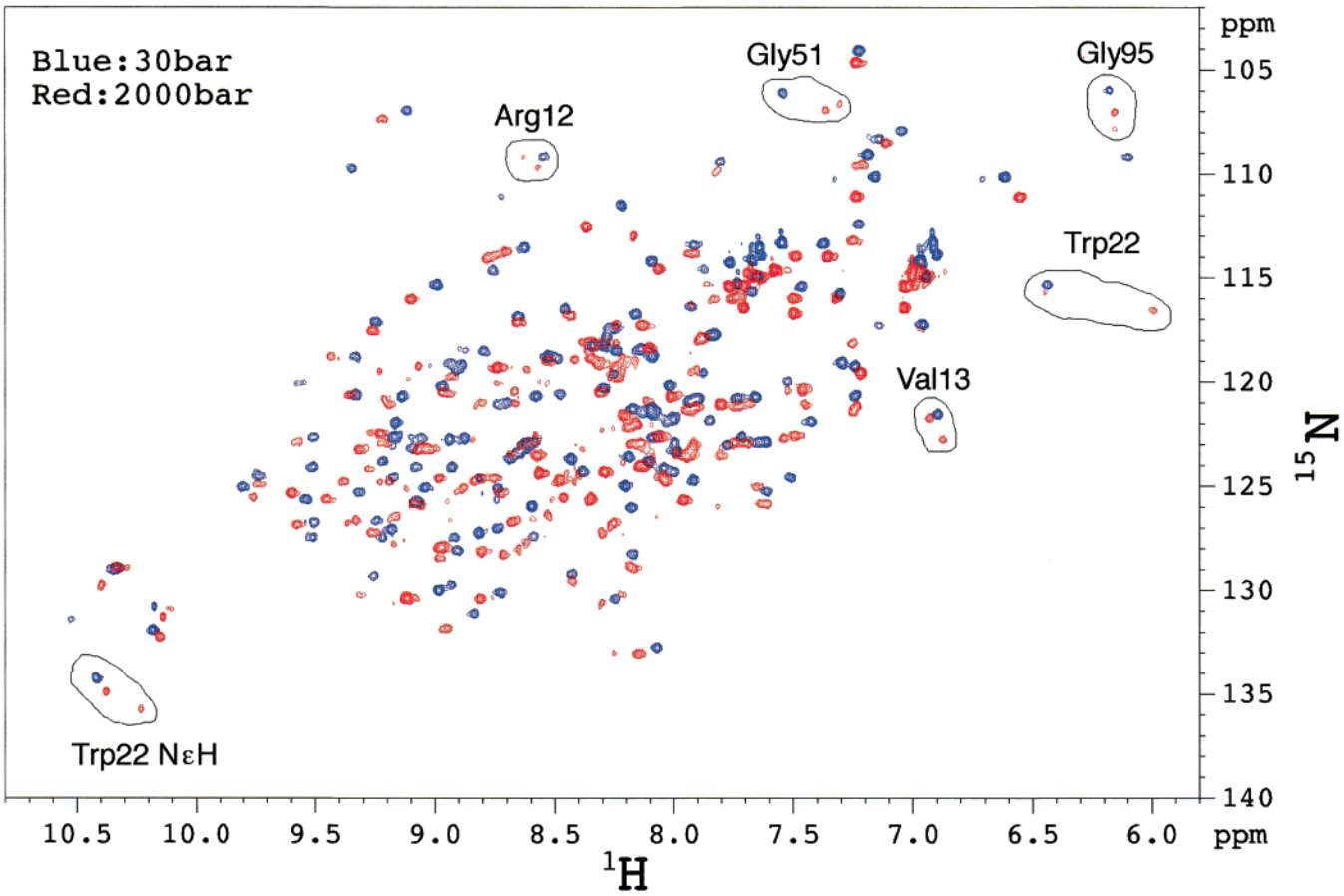

FIGURE 1: $^{15}N/^{1}H$ HSQC spectra of ^{15}N-uniformly labeled DHFR complexed with folate at 30 bar (blue) and at 2000 bar (red) at 15 °C. The protein is dissolved to a concentration of 1.2 mM in 20 mM Tris buffer (95% $^{1}H_2O$/5% $^{2}H_2O$, pH 7.0) containing 4.5 mM folate. Cross-peaks of Arg12, Val13, Trp22, Gly51, and Gly95 that split into two at high pressure are encircled.

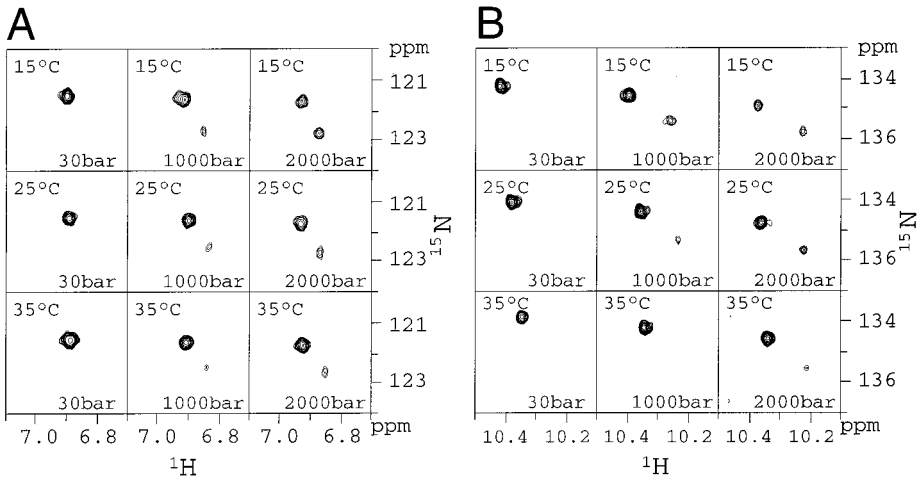

FIGURE 2: Expansion of the Val13-NH (A) and Trp22-NϵH (B) cross-peaks in the $^{15}N/^{1}H$ HSQC spectra of DHFR at various pressures and temperatures.

logarithm (Gibbs free energy change) against pressure (Figure 3B), we evaluated the volume difference between the two conformers, $\Delta V = V$ (second conformer) $- V$ (first conformer), to be -25 mL/mol using eq 1 (see Materials and Methods). A negative ΔV is usually encountered in a protein unfolding event (*11*) where part or all of the polypeptide segment is exposed to the solvent and is considered to be contributed by the loss of cavities (*21*, *22*) and by increased hydration (*23*, *24*). The smaller volume in the second conformer, therefore, suggests that its polypeptide chain is likely to lose some cavities and be more hydrated.

The linear extrapolation of the ΔG to 1 bar gives 5.2 kJ/mol for ΔG_0, predicting a population of the second conformer about 10% at 1 bar. Cross-peaks for ~10% population are often undetectable beyond the noise level in two-dimensional NMR spectra, because of the broadening effect in both dimensions. In addition, extra broadening may arise from exchange effect, which is enhanced at low population.

We also investigated the temperature effects on the equilibrium between the two conformers. The cross-peak intensities of the paired signals at 2000 bar are plotted as a function of temperature in Figure 3C. Again by taking the

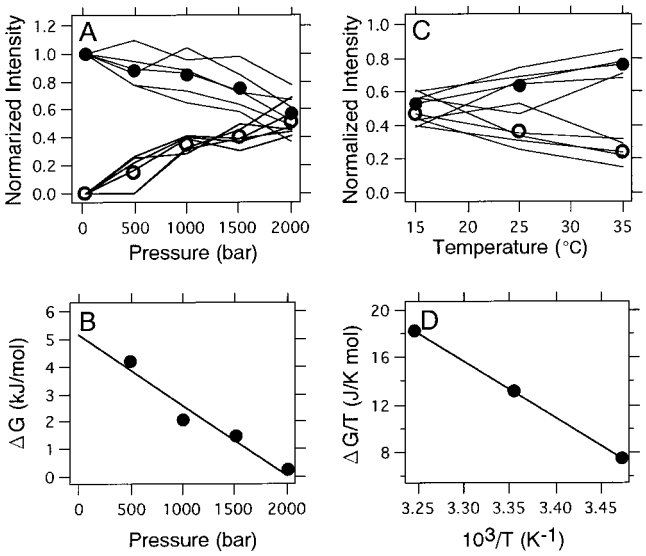

FIGURE 3: Estimation of thermodynamic parameters (ΔG, ΔV, ΔH, ΔS) for the equilibrium between the two conformers of DHFR. (A) Plots of normalized intensities of the split cross-peaks in the $^{15}N/^{1}H$ HSQC spectra against pressure for the peptide NH of Arg12, Val13, Trp22, Gly51, and Gly95 and the side chain NH of Trp22 at 15 °C. Filled and open circles give averages of the six values, from which equilibrium constants K are obtained. (B) Plots of the Gibbs energy difference (ΔG) between the two conformers against pressure. The slope gives ΔV from eq 1. (C) Plots of normalized intensities of the split cross-peaks in the $^{15}N/^{1}H$ HSQC spectra of DHFR against temperature for the peptide NH of Val13, Trp22, Gly51, and Gly95 and the side chain amide group of Trp22 at 2000 bar. Filled and open circles show averages of the five values, from which equilibrium constants K are obtained. (D) Plots of $\Delta G/T$ against reciprocal absolute temperature. The slope gives ΔH from eq 2.

Table 1: Thermodynamic Parameters for the Transition from the First Conformer to the Second in the DHFR−Folate Binary Complex[a]

pressure (bar)	ΔG (kJ/mol)	ΔH (kJ/mol)	ΔS (kJ/K mol)	ΔV (mL/mol)
1	5.2			−25
500	4.2			
1000	2.1	−48	−0.17	
1500	1.5			
2000	0.3	−38	−0.13	

[a] 20 mM Tris buffer, pH 7.0.

average equilibrium constant of the four residues (Val13, Trp22, Gly51, and Gly95) in Figure 3C, we replotted the corresponding values of $\Delta G/T$ against reciprocal temperature (eq 2, Figure 3D). Estimated ΔH and ΔS values both at 1000 and 2000 bar are listed in Table 1. The smaller enthalpy and entropy of the second conformer against the first also suggest that the second conformer is more hydrated than the first (*25*).

To determine the rates of exchange between the two conformers, ^{1}H NOESY and ROESY experiments were carried out. The protein concentration was 3.5 mM in 20 mM Tris buffer (pH 6.8 at 25 °C) containing 5% $^{2}H_2O$. However, we do not observe exchange cross-peaks in any of those five residues up to a mixing time from 20 to 700 ms between 25 and 35 °C. At 40 °C, the protein precipitated, making such measurements impossible. However, the line widths of the split cross-peaks of those five residues at 2000 bar were estimated, on average, to be 20 ± 5 Hz at 25 °C,

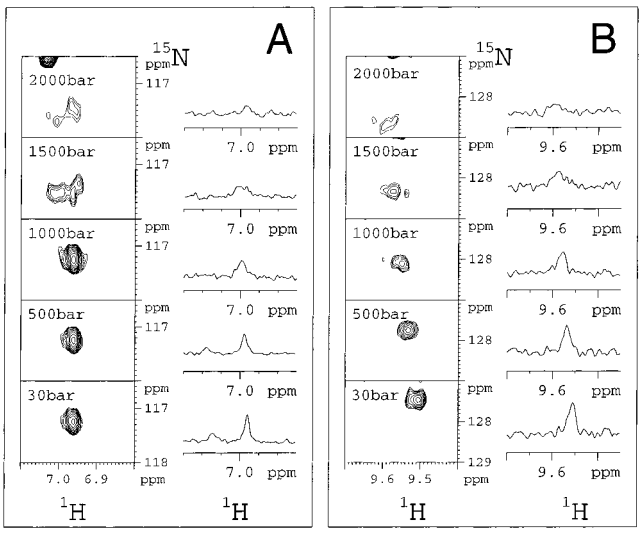

FIGURE 4: Pressure-dependence of $^{15}N/^{1}H$ HSQC spectra for the amide groups of Arg52 (A) and Leu54 (B) with ^{1}H cross sections at their ^{15}N resonance frequencies.

by fitting them with Lorentzian line shapes, giving the upper limits for the exchange rates to be 20 s^{-1}.

Besides the split of cross-peaks into two, many peaks lose their intensities with increasing pressure (Figure 1). In the spectral slices shown in Figure 4, panels A (Arg52) and B (Leu54), line broadening with increasing pressure is apparent, which would cause the loss of cross-peaks in the HSQC spectrum. The broadening would arise from such an NH group whose ^{15}N and ^{1}H chemical shifts differ only slightly between the first and the second conformers, so that their mutual shifts are not large enough to give separate signals but rather simply broaden due to slow conformational exchange between the two conformers. We found that the number of residues whose cross-peak intensities decrease by one-half is about 10.

Figure 5A shows a histogram of integrated cross-peak intensities in the $^{15}N/^{1}H$-HSQC spectra at 2000 bar, each normalized to that at 30 bar, against the amino acid sequence. A significant decrease in cross-peak intensity is observed for about 10 residues marked by green in Figure 5A. Figure 5B depicts the crystal structure of DHFR complexed with both folate and $NADP^{+}$, clearly showing the local segments of the protein involved in the NADPH binding, namely, the M20 loop, the C and F helices, and the region of residues 67−79. Superimposed on the stereo figures, the regions where the intensity at 2000 bar is less than half of that at 30 bar are color-coded green, while those giving the split signals are color-coded red. The decrease in cross-peak intensity (green) is considered to arise from the insufficiently split pair of cross-peaks and therefore to be also an indicator of the presence of the second conformer. Note that in Figure 5B the red and green-colored residues are on or close to the NADPH binding segments.

DISCUSSION

The X-ray crystallographic study of folate-bound DHFR (*1*) revealed two structures of the DHFR−folate binary complex under different crystallizing conditions. They correspond to two different conformations particularly in the M20 loop open and occluded, shown in Figure 5C (*1*). A

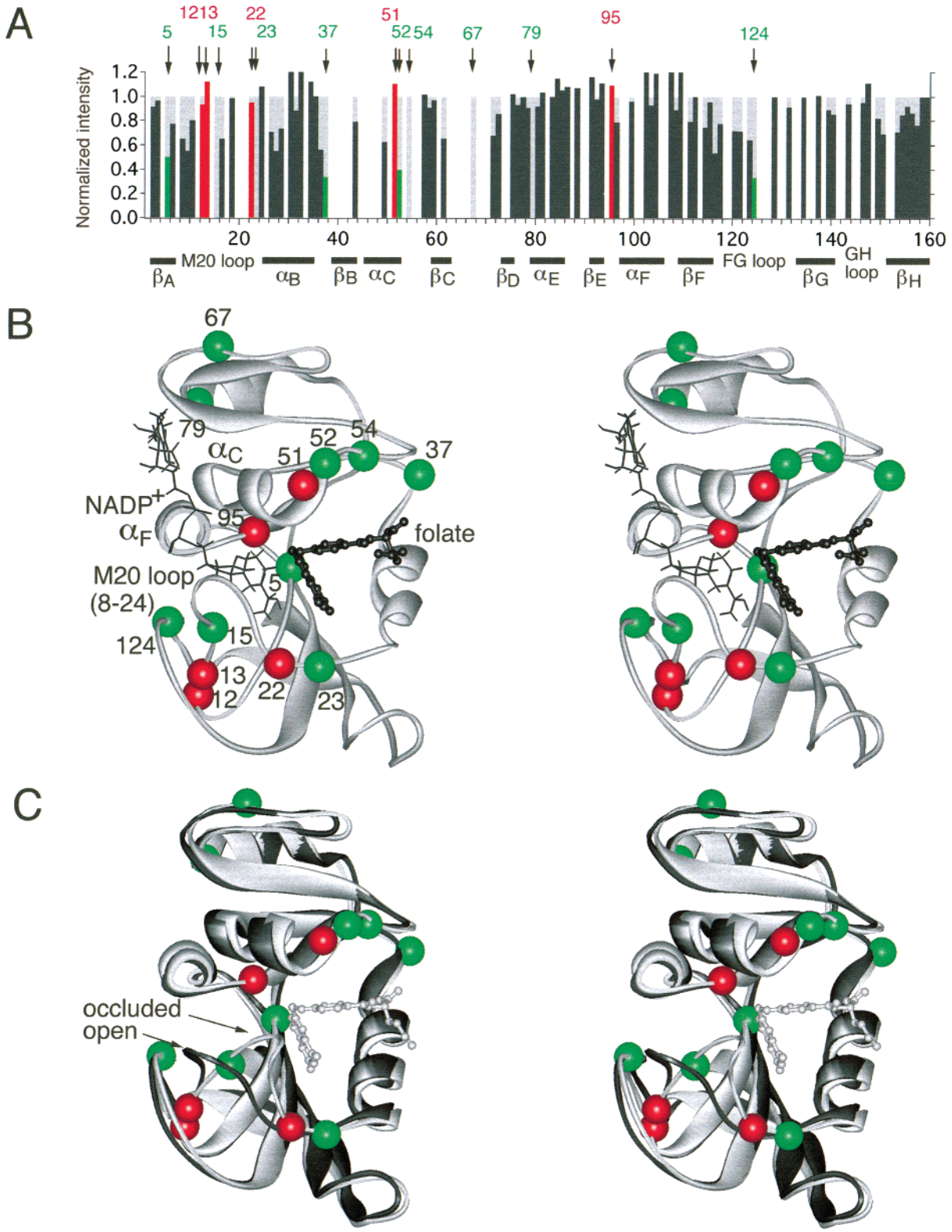

FIGURE 5: (A) Histograms of individual cross-peak intensities at 2000 bar in the $^{15}N/^{1}H$ HSQC spectra of DHFR complexed with folate against the amino acid sequence, each normalized to the intensity at 30 bar (gray). Red columns show residues giving split cross-peaks. Green columns show residues whose cross-peak intensities are decreased to less than 50% at 2000 bar. Open columns indicate no data. The location of the secondary structures are marked (PDB code: 1DYI). (B) Three-dimensional X-ray structure of the DHFR−folate−$NADP^+$ ternary complex (PDB code: 7DFR). The substrate folate is drawn by stick and ball, while the cofactor $NADP^+$ is drawn by wire frame. The figure shows that the NADPH binding site involves the M20 loop, the α_c and α_F helices, and the 67−79 loop. The five residues that show doublet splittings at 2000 bar in Figure 1 are marked by red spheres. Residues whose cross-peak intensities are decreased to less than 50% at 2000 bar are marked by green spheres. The actual experiment was carried out in the DHFR−folate binary complex (in the absence of $NADP^+$). (C) Two crystal structures of the DHFR−folate binary complex, the occluded form (gray, PDB code: 1RX7) and the open form (black, PDB code: 1RD7) (*1*).

somewhat similar conformational variation around the M20 loop was realized in a unit cell of folate-bound DHFR from *E. coli* (A-chain and B-chain) (*1*, *26*). In our present experiments, Arg12, Val13, and Trp22 show about 1 ppm split of ^{15}N cross-peaks at high pressure. These are located at both ends of the M20 loop. Also split are cross-peaks of Gly51 and Gly95, located near the ends of helices C and F (Figure 5B). ^{15}N chemical shift is determined by local electronic structure, and for a peptide amide group, the pressure-induced shift is correlated with changes in ϕ and ψ torsion angles beside changes in hydrogen bond geometry (*9*, *27*). As a measure of the extent of the angle changes, we may use the empirical equation for the β-sheet part of BPTI, $\Delta\delta_{15N} = -0.2325\psi$. Then, the observed ^{15}N chemical shift of about 1 ppm corresponds to a change in ψ angle of about 4 deg. The estimate suggests that the local torsion angles change considerably between the two conformers at these five residue sites. Apparently, the M20 loop and the C and F helices change orientation relative to other parts of the protein molecule, but local structural rearrangements involving changes in ϕ and ψ torsion angles would be small within these loop and helices, since no cross-peak splitting with significant differences in ^{15}N chemical shifts was observed but only broadening of cross-peaks of about 10 residues.

The picture of two conformers emerging from our pressure experiments may be compared with the open (black) and occluded (gray) forms of folate-bound DHFR determined in crystals (Figure 5C) (*1*). The residues giving split peaks and broadened peaks are color-coded red and green, respectively, on the occluded (gray) form in Figure 5, panel C, similarly as in Figure 5, panel B. The large torsion angle changes predicted for red-colored residues 12, 13, and 22 in solution clearly coincide with the large hinge motion of the M20 loop that takes place between the open (black) and occluded (gray) forms in crystals. Similar torsion angle changes predicted for red-colored residues 51 and 95 in solution are matched with the conformational changes of the C and F helices in the crystal (*1*). The coincidence suggests strongly that the first and the second conformers found in solution are close to the occluded and open conformers found in crystals.

The transition from the first conformer to the second is characterized with a negative volume change ($\Delta V = -25$ mL/mol), a negative enthalpy change ($\Delta H = \sim -43$ kJ/mol at 1000−2000 bar), and a negative entropy change ($\Delta S = \sim -0.15$ kJ/K mol at 1000−2000 bar), all of which suggest strongly that the transition is accompanied by increased hydration (*21*−*25*). In general, hydration is likely to be accompanied by decreased cavity formation (*21*, *22*). Calculation with a program GRASP (*28*) shows that the cavity volume decreases considerably in the transition from the occluded conformer to the open conformer in crystals ($\Delta V = -60$ to -15 mL/mol with probes of 1.0−1.3 Å radius).

In the present work, splitting of the cross-peaks at high pressure is attributed to the equilibrium of the two conformers. To confirm the generality of the method, we carried out a similar experiment on the DHFR complex with methotrexate, for which the existence of two equilibrium conformers at 1 bar has been established by ^{1}H NMR (*3*). In the ^{15}N-uniformly labeled DHFR complexed with methotrexate, we clearly detected a number of split ^{15}N/^{1}H HSQC cross-peaks at 1 bar, whose relative intensities vary continuously with pressure (data not shown). Thus, the existence of two conformers is not limited to the folate-bound form of DHFR but is likely to be a general design for a substrate (or analogue)-bound form of DHFR. The existence of the open conformer would be crucial for DHFR to bind its cofactor, since in the closed (or occluded) conformation the NADPH binding pocket is totally covered by the M20 loop, thereby eliminating the chance of NADPH binding. A relatively small fraction of the open conformer (at most ~10% in the DHFR−folate complex at 1 bar) would be sufficient for the efficient function of the protein, because the open and the closed (or occluded) conformers are in dynamic equilibrium concerted with the hinge motion. The rate of opening of the NADPH binding sites (estimated to be <20 s^{-1} at 2000 bar) would give the upper limit for the rate of NADPH binding.

CONCLUDING REMARKS

The present study shows that a conformational change of a protein from an occluded form to an open form is sensitively affected by pressure. The pressure sensitivity arises because such a change involves a significant decrease in partial molar volume of the protein, due partly to the loss of cavities and partly to the increased hydration of the segments involved. Loss of cavities and increased hydration in an open conformer are not restricted to DHFR but are expected to occur more generally in globular proteins. Combined with the multidimensional capability of the modern high-resolution NMR spectroscopy, pressure offers a novel means for exploring more open and hydrated forms of protein structure that might have direct relevance to function.

ACKNOWLEDGMENT

We thank Dr. Y. Ashida of Hiroshima University for the gift of *E. coli* BL21 strain. We also thank Dr. S. Izumi and Instrument Center for Chemical Analysis of Hiroshima University for the measurement of the mass spectra.

REFERENCES

1. Sawaya, M. R., and Kraut, J. (1997) *Biochemistry 36*, 586−603.
2. Epstein, D. M., Benkovic, S. J., and Wright, P. E. (1995) *Biochemistry 34*, 11037−11048.
3. Falzone, C. J., Wright, P. E., and Benkovic, S. J. (1991) *Biochemistry 30*, 2184−2191.
4. Li, L., Falzone, C. J., Wright, P. E., and Benkovic, S. J. (1992) *Biochemistry 31*, 7826−7833.
5. Falzone, C. J., Wright, P. E., and Benkovic, S. J. (1994) *Biochemistry 33*, 439−442.
6. Yamada, H. (1974) *Rev. Sci. Instrum. 45*, 640−642.
7. Akasaka, K., Tezuka, T., and Yamada, H. (1997) *J. Mol. Biol. 271*, 671−678.
8. Li, H., Yamada, H., and Akasaka, K. (1998) *Biochemistry 37*, 1167−1173.
9. Akasaka, K., Li, H., Yamada, H., Li, R., Thoresen, T., Woodward, C. K. (1999) *Protein Sci. 8*, 1946−1953.
10. Li, H., Yamada, H., and Akasaka, K. (1999) *Biophys. J. 77*, 2801−2812.
11. Lassalle, M. W., Yamada, H., and Akasaka, K. (2000) *J. Mol. Biol. 298*, 293−302.
12. Inoue, K., Yamada, H., Akasaka, K., Herrmann, C., Kremer, W., Maurer, T., Döker, R., and Kalbitzer, R. (2000) *Nat. Struct. Biol. 7*, 547−550.

13. Iwakura, M., and Tanaka, T. (1992) *J. Biochem. 111*, 31−36.
14. Ohmae, E., Iriyama, K., Ichihara, S., and Gekko, K. (1996) *J. Biochem. 119*, 703−710.
15. Fierke, C. A., Johnson, K. A., and Benkovic, S. J. (1987) *Biochemistry 26*, 4085−4092.
16. Bodenhausen, G., and Ruben, D. J. (1980) *Chem. Phys. Lett. 69*, 185−189.
17. Sklenar, V., Piotto, M., Leppic, R., and Saudek, V. (1993) *J. Magn. Reson., Ser. A. 102*, 241−245.
18. Kitamura, Y., and Itoh, T. (1987) *J. Solution Chem. 16*, 715−725.
19. Falzone, C. J., Benkovic, S. J., and Wright, P. E. (1990) *Biochemistry 29*, 9667−9677.
20. Falzone, C. J., Cavanagh, J., Cowart, M., Palmer, A. G., Matthews, C. R., Benkovic, S. J., and Wright, P. E. (1994) *J. Biomol. NMR 4*, 349−366.
21. Tamura, Y., and Gekko, K. (1995) *Biochemistry 34*, 1878−1884.
22. Frye, K. J., and Royer, C. A. (1998) *Protein Sci. 7*, 2217−2222.
23. Kauzmann, W. (1959) *Adv. Protein Chem. 14*, 1−63.
24. Weber, G., and Drickamer, H. G. Q. (1983) *Rev. Biophys. 16*, 89−112.
25. Makhatadze, G. I., and Privalov, P. L. (1994) *Biophys. Chem. 51*, 291−309.
26. Reyes, V. M., Sawaya, M. R., Brown, K. A., and Kraut, J. (1995) *Biochemistry 34*, 2710−2723.
27. Le H., Oldfield, E. (1994) *J. Biomol. NMR 4*, 341−348.
28. Nicholls, A., Sharp, K. A., and Honig, B. (1991) *Proteins 11*, 281−296.

BI0009993